Manuscript clean
Click here to download Manuscript ArtRes_paper_v14_cleanedup.docx

1 # Multi-omics based identification of specific biochemical changes
2 associated with PfKelch13-mutant artemisinin resistant *Plasmodium*
3 *falciparum*

4 Ghizal Siddiqui[1], Anubhav Srivastava[1], Adrian S. Russell[1] and Darren J. Creek[1*]

5 [1]Drug Delivery, Disposition and Dynamics, Monash Institute of Pharmaceutical Sciences, Monash
6 University, Parkville Campus, Parkville, Victoria, Australia.

7 * Corresponding author: Darren J. Creek, Drug Delivery, Disposition and Dynamics, Monash Institute
8 of Pharmaceutical Sciences, Monash University, Parkville Campus, Parkville, Victoria, Australia. Tel:
9 +61 (0) 3 9903 9249; Fax: +61 (0) 3 9903 9583; e-mail, Darren.creek@monash.edu

10 Key words: (3-10 key words) malaria, *Plasmodium falciparum*, artemisinin resistance, PfKelch13,
11 proteomics, metabolomics, peptidomics

12 Running head: Biochemical impact of PfKelch13 mutations

13 Word count (text): 3499

14 Word count (abstract): 174

15 Figures: 5

16 Tables: 2

17 References: 49

18 Summary

19 Multi-omics analyses of PfKelch13-mutant artemisinin resistant and sensitive *Plasmodium falciparum*
20 revealed artemisinin resistance to be associated with a two-fold decrease in PfKelch13 protein
21 abundance, decreased haemoglobin digestion and increased glutathione production.

22 ## Abstract

23 ***Background.*** The emergence of artemisinin resistance in the malaria parasite, *Plasmodium falciparum,* poses a
24 major threat to the control and elimination of malaria. Certain point mutations in the propeller domain of
25 *PfKelch13* are associated with resistance, but *PfKelch13* mutations do not always result in clinical resistance.
26 The underlying mechanisms associated with artemisinin resistance are poorly understood and the impact of
27 *PfKelch13* mutations on cellular biochemistry is not defined.

28 ***Methods.*** This study aimed to identify global biochemical differences between PfKelch13-mutant artemisinin –
29 resistant and –sensitive strains of *P. falciparum* by combining LC-MS-based proteomics, peptidomics and
30 metabolomics.

31 ***Results.*** Proteomics analysis found both *PfKelch13* mutations examined to be specifically associated with
32 decreased abundance of PfKelch13 protein. Metabolomics analysis demonstrated accumulation of glutathione
33 and its precursor, gamma-glutamylcysteine, and significant depletion of one other putative metabolite in
34 resistant strains. Peptidomics analysis revealed lower abundance of several endogenous peptides derived from
35 haemoglobin (HBα and HBβ) in the artemisinin resistant strains.

36 ***Conclusion.*** *PfKelch13* mutations associated with artemisinin resistance lead to decreased abundance of
37 PfKelch13 protein, decreased haemoglobin digestion and enhanced glutathione production.

38

39 # Introduction

40 Malaria is a major global health problem, with over 200 million cases of malaria and an estimated 429, 000
41 deaths in 2015 [1]. *Plasmodium falciparum* causes the most severe form of malaria and is responsible for the
42 highest incidence, especially in the WHO African Region where 90% of malaria cases and 92% of deaths due to
43 malaria occur [1].

44 Artemisinin-based combination therapy (ACT) has been the recommended treatment for *P. falciparum* malaria
45 since 2005, and has contributed to a significant reduction in malaria incidence and mortality [2]. However, the
46 prevalence of ACT failure is increasing, especially in South-East Asia. Resistance to ACT was first reported in
47 Western Cambodia and has now spread across the Greater Mekong Subregion, an area known historically for
48 the emergence of resistance against previous first-line antimalarials [3]. The spread of chloroquine resistance
49 from South-East Asia to Africa had significant implications for malaria control, and the emergence of
50 artemisinin resistance in Africa could have devastating consequences.

51 Clinically, artemisinin resistance is defined by slow parasite clearance in *P. falciparum*-infected patients post-
52 treatment [3] and is associated with an increased survival of ring-stage parasites after short-term exposure to
53 artemisinin *in vitro* [4, 5]. Recently, point mutations in the propeller domain of the *PfKelch13* gene
54 (PF3D7_1343700) were shown to be associated with resistance to artemisinin *in vitro* and *in vivo* in South-East
55 Asian *P. falciparum* strains [6-8]. To date, a total of 186 different *PfKelch13* alleles have been reported in Asia
56 [9], but only a small subset of these mutants have been shown to be associated with artemisinin resistance [7, 8,
57 10-12], with four of these mutations (Y493H, R539T, I543T and C580Y) further confirmed *in vitro* [6, 8, 13].
58 Furthermore, mutations in the *PfKelch13* gene have not yet been identified to be associated with artemisinin
59 resistance in African *P. falciparum* strains [14-19].

60 The use of *PfKelch13* as a genetic molecular marker for artemisinin resistance is time-consuming and not
61 always predictive of treatment outcome [9]. Additionally, labour intensive *in vitro* assays are required for
62 confirmation of resistance [19, 20]. An alternative set of biomarkers of artemisinin resistance would be valuable
63 for epidemiological monitoring, and potentially for point-of-care testing to assist with drug selection.

64 The genetic mutations responsible for artemisinin resistance likely mediate specific biochemical functions that
65 help to define the resistance phenotype [21]. In this study, differences in the biochemical phenotype of three

66 pairs of *PfKelch13*-mutant parasites and relevant controls were characterised by analysing their global
67 proteome, metabolome and peptidome.

68 This integrative multi-omics approach identified putative biomarkers that were consistently associated with
69 artemisinin resistant *PfKelch13* mutants, including the PfKelch13 protein, glutathione-related metabolites and
70 endogenous peptides derived from haemoglobin.

71 # Methods

72 ## *P. falciparum* parasite culture

73 All *P. falciparum* strains were cultured as previously described [22] and all analyses were performed within six
74 weeks of the parasites being thawed. Parasites were tightly synchronised by double treatment with sorbitol and
75 when required, magnetic column purification was performed to obtain highly-enriched trophozoite stage
76 infected red blood cells (iRBCs) as described previously [23, 24]. The artemisinin resistant and sensitive *P.*
77 *falciparum* isolates used in this study included two common *PfKelch13* mutants and the *PfKelch13* wild-type on
78 an isogenic background [13], and two field strains [25] (Table 1). Global proteomic analyses were performed
79 on ring and trophozoite stage parasites, but global metabolomics and peptidomics analyses were focussed only
80 on trophozoite stage parasites.

81 ## Global proteomic studies

82 *Proteomics sample preparation*

83 Intracellular parasites were purified from iRBCs using 0.1% saponin as described previously [26]. Parasite
84 pellets were solubilised with lysis buffer (100 mM HEPES, 1% sodium deoxycholate (SDC), pH 8.1)
85 supplemented with phosphatase and protease inhibitors for 5 min at 95 °C. Proteins were reduced, alkylated and
86 then precipitated with trichloroacetic acid (TCA). The supernatants were kept for peptidomics sample
87 preparation. The pellets were resuspended in 1 ml of lysis buffer and then 500-800 µg of total protein
88 (accurately determined using Pierce BCA protein assay kit (Thermo Scientific™ Pierce™)) was incubated
89 overnight with trypsin (Promega) (1:50). On the following day, dimethyl duplex labelling was performed [27].
90 After labelling, protein samples from the resistant and sensitive lines were mixed and the peptide mixture was
91 fractionated using a disposable Strong Cationic exchange solid phase extraction cartridge (Agilent Bond Elut).
92 Eluates (fractions) and flowthroughs collected were subjected to desalting using in-house generated StageTips
93 as described previously [28]. The fractions were then dried and resuspended in 20 µL of 2% (v/v) acetonitrile
94 (ACN) and 0.1% (v/v) formic acid (FA) for LC-MS/MS analysis.

95 *Proteomics LC-MS/MS analysis and data processing*

96 LC-MS/MS was performed using an Ultimate U3000 Nano LC system (Dionex) and Q Exactive™ Hybrid
97 Quadrupole-Orbitrap Mass Spectrometer (ThermoFisher®). Samples were loaded at a high flow rate onto a

98 reversed-phase trap column (100 µm x 2 cm) Acclaim PepMap media (Dionex) in 0.1 % (v/v) FA in water.
99 Peptides were eluted from the trap column at a flow rate of 0.3 µl/min through a reversed-phase capillary
100 column (75 µm x 15 cm) (LC Packings, Dionex) into the nanospray ion source of the mass spectrometer (MS).
101 For proteomics analysis, the HPLC gradient was set to 115 min using a gradient that reached 30% ACN after 55
102 min, then 45% after 85 min, 55% after 90 min and 90% after 100 min. The MS was operated in a data-
103 dependent mode with 2 microscan FTMS scan events at 70,000 resolution (MS) over the *m/z* range of 375-1800
104 Da in positive ion mode, and up to 20 data-dependent HCD MS/MS scans.

105 Identification and quantification of proteins was performed using MaxQuant proteomics software [29].
106 Statistical analysis for the determination of differential proteins used parametric and non-parametric hypothesis
107 testing, and a linear model approach. Log-transformed fold-difference for paired artemisinin resistant and
108 sensitive samples and one sample t-test were calculated in MS-Excel to test the mean of combined experiment
109 groups against the known mean ($\mu = 0$) [30]. Bonferroni correction was applied to the significance threshold to
110 adjust for multiple testing. Rank Product analysis, a non-parametric permutation test, was conducted on the Log-
111 transformed fold-difference for paired artemisinin resistant and sensitive samples using the RankProd R package
112 [31]. The significance of each protein was assessed by the p-value and false discovery rate (FDR). Limma
113 analysis, a linear model designed to assess differential expression, was conducted using the limma R package
114 [32]. The significance of each protein was assessed by the p-value and adjusted p-value (adjusted for multiple
115 testing) calculated with the empirical Bayesian framework applied to the linear model.

116 Global metabolomics studies

117 *Metabolomics Sample preparation*

118 *P. falciparum* parasites were synchronised using sorbitol 24 hr before parasite harvest for metabolomics
119 experiments. A control culture containing only uninfected RBCs was also analysed. Metabolites were extracted
120 from magnetically enriched parasites (5 x 10^7) at 60-70% parasitaemia using cold methanol as previously
121 described [33]. Insoluble precipitates were removed by centrifugation and 100 µL of metabolite extract was
122 transferred to glass LC-MS vials and stored at -20 °C until analysis. An aliquot (20 µL) of each sample was
123 combined to generate a pooled biological sample for quality control (QC) procedures.

124 *Metabolomics LC-MS analysis and data processing*

125 Hydrophilic interaction liquid chromatography (ZIC-pHILIC, Merck) coupled to high resolution-mass
126 spectrometry (Q Exactive™, ThermoFisher®) was used to analyse metabolomics samples as before [34].
127 Approximately 250 metabolite standards were analysed immediately preceding the batch run to determine
128 accurate retention times to facilitate metabolite identification. Additional retention times for metabolites lacking
129 authentic standards were predicted computationally as previously described [35]. Identification and
130 quantification of metabolites was performed using the IDEOM workflow [36] and peak areas for significant
131 metabolites were confirmed by manual integration of raw LC-MS data with TraceFinder™ (ThermoFisher®).

132 LC-MS peaks heights, representing metabolite abundances, were normalised according to the median identified
133 peak for each sample. Univariate statistical analysis was done using IDEOM and Welch's t-test [36].
134 Multivariate statistical analysis utilised partial least squares - discriminant analysis (PLS-DA) and was applied
135 to log-transformed and auto-scaled data using the web-based analytical tool, MetaboAnalyst [37].

136 Global peptidomics studies

137 *Peptidomics sample preparation*

138 Supernatants collected post TCA precipitation from proteomics sample preparations were subjected to
139 centrifugal filtration (10 kDa cut-off, Amicon Ultra). The flow-through was collected and an equal amount of
140 ethyl acetate was added to remove residual SDC. Equal quantities of total peptides (50-70 µg by BCA) were
141 then used for peptidomics analyses. Peptide samples were subjected to desalting [28], and were then dried and
142 resuspended in 20 µL of 2% (v/v) ACN and 0.1% (v/v) FA for LC-MS/MS analysis.

143 *Peptidomics LC-MS/MS analysis and data processing*

144 LC-MS/MS was performed using the same methodology as the proteomics LC-MS/MS analysis (described
145 above and in supplementary methods) with minor modifications. Mass identification with +1 and up to +8
146 charge was also enabled.

147 Peptide identification was conducted with *de novo* sequencing assisted database search using PEAKS DB
148 software [38]. The identified peptide sequences from the *Homo sapiens* and *P. falciparum* proteome databases
149 that were detected in multiple samples were shortlisted. The mass to charge ratio and retention time of 148
150 shortlisted peptides were imported into TraceFinder™ (ThermoFisher®) and the peak intensity was obtained by

151 manually adjusting the integration and accounting for retention time drift when required. Log-transformed fold-
152 difference and Welch's t-test were calculated in MS-Excel for paired artemisinin resistant and sensitive samples.

153 # Results

154 This study combined metabolomics, peptidomics and proteomics (Figure 1) to identify novel potential
155 biomarkers for *PfKelch13* mutant *P. falciparum* isolates associated with artemisinin resistance. Resistant and
156 sensitive *P. falciparum* parasite isolates (Table 1) were synchronised and grown *in vitro* to the equivalent stage
157 of the intra-erythrocytic cycle (rings: 6-12 hours post invasion (hrs p.i), trophozoites: 24- 30 hrs p.i), followed
158 by parallel extractions for metabolomics, peptidomics and proteomics analysis by LC-MS (Figure 1).

159 ## Quantitative dimethyl-based proteomic analysis

160 Global proteome analysis was performed using reductive dimethyl labelling to identify quantitative differences
161 in protein levels between artemisinin sensitive and resistant *P. falciparum* isolates. Two clonal artemisinin
162 resistant isolates with defined *PfKelch13* mutations (Cam3.II^{R539T} and Cam3.II^{C580Y}) were compared to their
163 isogenic *PfKelch13* wild-type strain (Cam3.II^{rev}) [13] and two independent field isolates from the Pailin region
164 of Cambodia, a *PfKelch13*-mutant artemisinin resistant isolate (PL7) and *PfKelch13* wild-type sensitive (PL2)
165 isolate [25] were compared to each other (Table 1).

166 Saponin lysed ring-stage parasite proteins from Cam3.II^{R539T} and Cam3.II^{rev} were labelled for quantitative
167 proteomics from three biological replicates. Ring stage parasites were chosen for initial proteomic analysis, as
168 this is the stage where differential *in vitro* sensitivity to artemisinin has been reported [6-8]. A total of 920
169 proteins were identified with at least two unique peptides, with 432 proteins in common between the three
170 replicates (Supplementary data file 1). Compared with the control, a significant reduction in the abundance of
171 six proteins was observed ($p \leq 0.05$; log fold-change > 0.5), including the PfKelch13 protein itself (Figure 2), and
172 only one protein, Pf13_0341, a putative DNA-directed RNA polymerase 2, was significantly more abundant in
173 the resistant strain (Supplementary data file 1). It was noted that the ring-stage proteomics data demonstrated
174 relatively poor coverage and high variability, likely due to the challenges associated with purification of ring-
175 stage parasites following saponin lysis. Whilst decreased ring-stage sensitivity to artemisinins is the accepted *in*
176 *vitro* model for artemisinin resistance, decreased sensitivity has also been reported for trophozoite stages when
177 treated for a short duration (< 2 h) [25], suggesting that the resistance mechanism is not stage-specific.
178 Therefore, further studies were performed on trophozoite-stage parasites, allowing improved reproducibility and
179 purity from uninfected RBC contaminants.

180 For trophozoite stage parasites, a total of 2824 proteins were identified from three to four biological replicates of
181 three pairs of parasite strains (Supplementary data file 1). Data from all eleven experiments were combined in
182 order to detect significant proteins associated with all three resistant strains tested, and three types of statistical
183 tests were applied to minimise the likelihood of false discoveries. As the rank product analysis performs poorly
184 with data sets containing missing values, the data set was restricted to proteins detected in all eleven
185 experiments, resulting in a set of 520 proteins for analysis. The limma analysis was also conducted on an
186 expanded data set of 1133 proteins that were detected in at least one experiment for each of the three pairs of
187 parasite strains and the same significant proteins were identified (data not shown). Only five proteins were
188 apparently different (p-value < 0.05) according to each of the statistical tests applied (Table 2). However, when
189 taking multiple testing corrections for all three tests into account (Bonferroni correction for t-test, FDR for rank
190 product analysis and adjusted p-value for limma), only PfKelch13 abundance was found to be significantly
191 different across all parasite strains (Table 2). PfKelch13 abundance was approximately two-fold lower in the
192 resistant strain across all 14 individual experiments including ring and trophozoite-stage parasites (Figure 3A).
193 The identification of PfKelch13 was confidently assigned based on the detection of 20 unique peptides, and
194 manual analysis of the data confirmed lower abundance of peptides from both the N-terminal region and the C-
195 terminal propeller domain in resistant (*PfKelch13*-mutant) compared to the sensitive (wild-type) strains (Figure
196 3B).

197 Metabolomics analysis of artemisinin resistant parasites

198 Comparative untargeted metabolomics was used to investigate the impact of resistance-associated *PfKelch13*
199 mutations on the metabolome of two clonal resistant lines Cam3.II^{R539T} and Cam3.II^{C580Y}, relative to the
200 sensitive line Cam3.II^{rev} (n = three biological replicates). Univariate statistical analysis of all identified
201 metabolite features revealed few significant differences between the wild-type and both mutant lines.
202 Supervised multivariate analysis (PLS-DA) revealed a combination of metabolic features in the second
203 component (PC2) that were associated with resistance (Figure 4A). Detailed analysis of this model revealed four
204 metabolites with VIP scores above 0.3, and subsequent manual integration of LC-MS data for these features
205 confirmed that one metabolite was significantly depleted in the resistant lines, and three were more abundant
206 (Figure 4B). Levels of glutathione, and its precursor gamma-glutamylcysteine, were 74%, and 57%, higher in
207 the resistant parasites than sensitive, respectively. Levels of NAD+ were only 20% higher in the resistant
208 parasites than sensitive. The depleted metabolic feature in both resistant strains was putatively identified as L-

209 proline amide. This metabolite was detected in the uninfected RBCs, and is likely derived from the host cells
210 (Supplementary data file 2).

211 Peptidomics analysis of artemisinin resistant parasites

212 Proteolysis is an important biochemical function in *P. falciparum*, and degradation of parasite (via the
213 proteasome) and host (via the digestive vacuole) proteins has been proposed to influence the mechanism of
214 action and/or resistance of artemisinin [39]. Most endogenous peptides liberated by protein digestion processes
215 are not detected on the standard metabolomics and proteomics methods, necessitating the incorporation of a
216 dedicated peptidomics analysis to investigate these proteolytic pathways. Peptidomics analysis identified 146
217 endogenous peptides that aligned with proteins from the *P. falciparum* (68 peptides) and *H. sapiens* (78
218 peptides) databases (Supplementary data file 3). Significant reductions in the abundance of 19 peptides were
219 observed in artemisinin resistant lines compared to their appropriate controls ($p \leq 0.05$; log fold-change > 0.5),
220 including eight peptides that originated from Hbβ, ten originated from Hbα (Figure 5) and one originated from
221 another *H. sapiens* protein, Uniprot ID number POU3F3 (Supplementary data file 3). No significant differences
222 in the abundance of *P. falciparum*-derived peptides were observed.

223 ## Discussion

224 Integrative multi-omics approaches provide a comprehensive analysis of the abundance of cellular biochemicals,
225 which can help in understanding the mechanism of artemisinin resistance. In this study, the proteomic,
226 peptidomic and metabolic profiles of artemisinin resistant *P. falciparum* strains were investigated to reveal the
227 biochemical impact of artemisinin resistance-associated *PfKelch13* mutations. The multi-omics analysis
228 revealed that *PfKelch13* mutations do not have a widespread impact on the biochemistry of *P. falciparum* under
229 standard *in vitro* culture conditions. The abundance of PfKelch13 protein itself was found to be consistently
230 lower in all the resistant lines compared to the sensitive strains. Endogenous peptides originating from
231 haemoglobin, and one putative host-derived metabolite, were also decreased in abundance, while levels of
232 glutathione and gamma-glutamylcysteine were higher in artemisinin resistant lines compared to the *PfKelch13*
233 wild-type, artemisinin-sensitive, controls.

234 Artemisinin resistance is associated with point mutations on the *PfKelch13* allele. The exact function of
235 PfKelch13 is not yet known, however, the C-terminal propeller domain shows homology to the human Keap1
236 protein, whose main function is to respond to oxidative stress by regulating levels of the transcription factor
237 Nrf2 [6, 40]. Interestingly, the global proteomics analysis of ring and trophozoite parasite stages in both
238 artemisinin resistant laboratory-generated clonal lines and field isolates identified decreased abundance of
239 PfKelch13 protein as the only significant differentiating feature (Figures 2 and 3, Table 2). Whilst no Nrf2
240 homologue has been identified in *P. falciparum*, based on Keap1 function, it is plausible that lower levels of
241 PfKelch13 protein in artemisinin resistant parasites would decrease the Kelch-mediated negative regulation of
242 the stress response, thereby making parasites more resilient to drug-induced oxidative stress. The observed
243 increase in glutathione abundance supports this hypothesis. It has also been hypothesised that the PfKelch13
244 protein is involved in the ubiquitination and proteasomal degradation of proteins within the endoplasmic
245 reticulum and is involved in the correct folding of proteins within the parasite [39]. In this case it is anticipated
246 that depletion of PfKelch13 protein in artemisinin resistant parasites would be associated with a dysregulated
247 unfolded protein response, which is consistent with the previously reported increase in mRNA expression of
248 genes associated with unfolded protein response [41], although no difference in abundance of those proteins was
249 observed in the untreated *in vitro* conditions described here (Supplementary data file 1).

250 Whilst the link between *PfKelch13* mutations and artemisinin resistance is well-established, *PfKelch13*
251 expression was not previously associated with artemisinin resistance [41], suggesting that the differential protein

252 abundance observed here may arise due to decreased translation, or enhanced degradation of the PfKelch13
253 protein, rather than transcriptional regulation. It has previously been demonstrated that artemisinin resistance in
254 laboratory-generated *PfKelch13*^{C580Y} mutant parasites (NF54 strain) is associated with an increased abundance
255 of *P. falciparum* phosphatidylinositol-3-kinase (PfPI3K) and its lipid product phosphatidylinositol-3-phosphate
256 (PI3P), likely due to a deficiency in PfKelch13-mediated ubiquitin-dependent degradation of PfPI3K [42]. This
257 hypothesis is consistent with the decreased abundance of PfKelch13 observed here, albeit these studies are
258 based on parasites with different genetic backgrounds. Unfortunately this untargeted metabolomics and
259 proteomics approach was not capable of detecting PI3P and PfPI3K (Supplementary data files 1 and 2). Other
260 published untargeted proteomics studies of blood stage *P. falciparum* have also failed to detect peptides from
261 PfPI3K in the absence of phosphopeptide enrichment [43]. Nevertheless, this study was able to successfully
262 demonstrate the specific impact of two common *PfKelch13* mutations (C580Y and R539T) on PfKelch13
263 protein abundance and suggest that there is potential to develop a quantitative biomarker assay for artemisinin
264 resistance that is independent of the specific *PfKelch13* genotype. Further studies on diverse *PfKelch13*
265 genotypes are necessary to confirm the association between PfKelch13 protein abundance and clinical
266 artemisinin resistance.

267 Whilst the *PfKelch13* mutant parasites did not exhibit significant changes to the proteome (beyond PfKelch13)
268 under these *in vitro* conditions, enhanced levels of glutathione and its precursor, gamma-glutamylcysteine, were
269 observed in the metabolomics analysis. Glutathione is a co-factor required for detoxification enzymes such as
270 glutathione peroxidase and glutathione S-transferase and its abundance is suggestive of the parasite's ability to
271 defend itself against additional oxidative stresses, such as that induced by artemisinin treatment [25, 44]. It has
272 been proposed that artemisinin resistant parasites are able to better manage oxidative damage [39], and
273 increased glutathione concentration been reported in rodent models of artemisinin-resistance [45, 46].

274 Our global peptidomics analysis identified a number of endogenous peptides originating from haemoglobin
275 (alpha and beta subunits) that were decreased in abundance in the resistant lines (Figure 5), suggesting down-
276 regulation of haemoglobin uptake or digestion. This decrease in haemoglobin catabolism could result in
277 decreased production of haem, which is necessary to activate artemisinin in order to mediate parasite killing.
278 Disrupted haemoglobin digestion and endocytosis has previously been demonstrated in artemisinin resistant
279 rodent parasites [45, 47]. The decreased haemoglobin digestion could be associated with quiescence, or a higher
280 proportion of ring stage parasites in the samples. However, the highly similar proteomics and metabolomics

281 profiles observed here confirmed that all samples were correctly normalised and at the same lifecycle stage at
282 the time of analysis, as stage-specific profiles would have been anticipated if significant differences in
283 development were apparent [48]. Dysregulation in the abundance of haemoglobin-derived peptides in
284 chloroquine-resistant *P. falciparum* lines has previously been reported [49]. However, chloroquine resistance
285 was associated with peptide accumulation, and it is therefore unlikely that haemoglobin-derived peptides will
286 provide a sensitive and selective biomarker in the context of multi-drug resistance.

287 In conclusion, through a combined proteomics, metabolomics and peptidomics analysis, the present study
288 revealed the effect of *PfKelch13* mutations on protein expression, metabolic pathways and endogenous peptide
289 levels in artemisinin-resistant lines compared to their sensitive (*PfKelch13* wild-type) controls. The functional
290 consequences of *PfKelch13* mutations were observed in the form of decreased haemoglobin digestion and
291 increased glutathione production. The abundance of PfKelch13 protein was two-fold lower in artemisinin
292 resistant *PfKelch13* mutants, and reproducible perturbations in the levels of other proteins were not observed.
293 Further validation in field isolates is necessary to determine the potential of PfKelch13 to be developed as a
294 quantitative biomarker for rapid diagnostic testing and monitoring resistance.

295 Acknowledgements

296 The Australian Red Cross Blood Service in Melbourne is gratefully acknowledged for providing human
297 erythrocytes used for *in vitro* cultivation of *P. falciparum* parasites. We thank Prof. David Fidock for the
298 genetically modified Cambodian isolates and Prof. Leann Tilley for field-derived Pailin isolates. Carson Yuan
299 assisted with the data analysis workflow for peptidomics analysis.

300 Authorship Contributions

301 GS performed experiments; GS, AS, and AR analysed results and made figures; GS and DJC designed the
302 research; GS, AS, and DJC wrote the manuscript; DJC directed the overall research program.

303 Conflicts of interest

304 All authors declare no competing financial interests.

305 Funding

306 DJC is funded by a National Health and Medical Research Council Career Development Fellowship
307 (APP1088855)

308 Presented in part: VIIN Young Investigator Symposium, Melbourne, Victoria, Australia, 14th October 2016.

309 American Society of Tropical Medicine and Hygiene Annual Meeting, Atlanta, GA, USA, 14th November 2016.

310 # Figure Legends

311 **Figure 1. Flow chart of the integrative multi-omics approach (metabolomics, proteomics and**
312 **peptidomics) used for the analysis of *P. falciparum* infected red blood cells (iRBCs).** For metabolomics
313 (indicated in black boxes) equal number of 5x 10^7 cells were used for metabolite extractions, samples were
314 analysed using LC-MS and data was processed using IDEOM. For peptidomics (indicated in light grey boxes
315 and arrows) an equal amount of peptides (50-70 µg) was used for analysis using LC-MS/MS and data was
316 processed and quantitatively analysed using PEAKS. For proteomics (indicated in grey boxes) equal amount of
317 total protein (500-800 µg) was labelled using reductive dimethyl labelling for quantitative analysis. Samples
318 from artemisinin resistant and sensitive iRBCs were then analysed using LC-MS/MS and the data was processed
319 and analysed using Maxquant.

320 **Figure 2. Volcano plot of ring-stage protein abundance in Cam3.II^{R539T} compared to Cam3.II^{rev}.** Log_2 fold
321 changes (x-axis) and T-test *p*-values (y-axis) of all proteins in ring stage parasites (6-12 hour post invasion).
322 Protein names are labelled next to significantly-different proteins.

323 **Figure 3. PfKelch13 is consistently and significantly down-regulated in artemisinin resistant lines**
324 **compared to their relevant controls.** (A) Relative abundance (Mean ± standard deviation) of PfKelch13 in
325 three different artemisinin resistant lines compared to their appropriate controls (see Table 1). (B)
326 Representative raw MS spectra of tryptic peptides from a 1:1 mixture of Cam3.II^{R539T}/PL7 (heavy labelled) and
327 control and Cam3.II^{rev}/PL2 (light labelled) extracts. The tryptic peptides (190-FSTVNNVNDTYEK-202, 623-
328 SSGAAFNYLNQIYVVGGIDNEHNILDSVEQYQPFNKR-659, 717-FGHSVLIANI-726), belonging to N- and
329 C-terminal regions of PfKelch13, show approximately two-fold lower relative abundance for the heavy-labelled
330 peptides compared to light-labelled peptides.

331 **Figure 4. Differentially abundant metabolites in artemisinin resistant (Cam3.II^{R539T} and Cam3.II^{C580Y})**
332 **versus artemisinin sensitive (Cam3.II^{rev}) lines.** (A) Multivariate analysis (PLS-DA) of all putative metabolite
333 features detected in Cam3.II^{R539T}, Cam3.II^{C580Y} and Cam3.II^{rev}. Sample projection (3 groups) onto the first PLS-
334 DA discriminant plane of Cam3.II^{rev} and Cam3.II^{R539T}, Cam3.II^{C580Y}. (B) Relative abundance of the four most

335 differentially abundant metabolites from iRBCs in two artemisinin resistant (Cam3.II^{R539T}, Cam3.II^{C580Y}) lines
336 compared to the control (Cam3.II^{rev}). Data are presented as mean ± standard deviation (n=3).

337 **Figure 5. Differentially abundant endogenous peptides originating from Hb in artemisinin resistant vs**
338 **artemisinin sensitive lines.** (A and C) Sequence coverage of Hbα and Hbβ from peptidomics analysis of
339 resistant lines compared to sensitive. The black bars represent endogenous peptides identified that were not
340 significantly different in abundance. The red bars represent endogenous peptides identified that were
341 significantly decreased in abundance in the resistant lines compared to sensitive, statistical analysis is shown in
342 supplementary data file 3. (B and D) Chromatograms from all detected Hbα and Hbβ peptides in
343 Cam3.II^{C580Y}versus Cam3.II^{rev}, PL7 versus PL2, and Cam3.II^{R539T} versus Cam3.II^{rev}. The chromatograms
344 demonstrated an overview of the decrease in abundance of peptides identified from Hb in the resistant lines
345 (above axis) compared to the sensitive (below axis).

346 **Table 1. *P. falciparum* strains used in this study.** Parasite strains, their response to artemisinin determined using *in vitro* ring-stage assay 0 to 3 hours/3 hours (RSA_{0-3h}/RSA_{3h}), *PfKelch13* genotype, identifying description and geographical source are listed.

Strain name	Response to artemisinin (700nM)	*PfKelch13* Genotype	Identifying description	Geographical source
Cam3.II^{rev}	0.7% survival using an *in vitro* RSA_{0-3h}	Wild-type	Cam3.II^{rev}, isogenic derivative of Cam3.II^{R539T}	Pursat province, Cambodia [13]
Cam3.II^{R539T}	49% survival using an *in vitro* RSA_{0-3h}	R539T	Cam3.II^{R539T}, parent of Cam3.II^{rev} and Cam3.II^{C580Y}	
Cam3.II^{C580Y}	24% survival using an *in vitro* RSA_{0-3h}	C580Y	Cam3.II^{C580Y}, isogenic derivative of Cam3.II^{R539T}	
PL2	5% minimum viability using an *in vitro* RSA_{3h}	Wild-type	Pailin- PL2, field isolate (genetically distinct from PL7)	Western Cambodia [25]
PL7	20% minimum viability using an *in vitro* RSA_{3h}	R539T	Pailin- PL7, field isolate (genetically distinct from PL2)	

348

349 **Table 2. List of *P. falciparum* proteins differentially regulated in expression in trophozoite stage parasites of artemisinin resistant (Cam3.II^{R539T}, Cam3.II^{C580Y}, PL7)**
350 **compared to artemisinin sensitive (Cam3.II^{rev} and PL2).** Mean relative abundance ± standard deviation, Student's t-test p-value, Rank Products p-value and false
351 discovery rate, limma p-value and adjusted limma p-value are shown, n= (11). PfKelch13 is the only protein significantly down-regulated in artemisinin resistant lines
352 according to all three analyses after adjustment for multiple testing ($p < 0.05$). *Less than Bonferroni-corrected p-value threshold ($\alpha = 4.03 \times 10^{-5}$).

Proteins differentially regulated in expression in trophozoite stage artemisinin resistant (Cam3.II^{R539T}, Cam3.II^{C580Y}, PL7) compared to artemisinin sensitive (Cam3.II^{rev} and PL2)								
Uniprot/PlasmoDB ID	**Protein**	**N**	**Mean±Std**	**Student's t-test p-value**	**Limma p-value**	**Rank product p-value**	**Rank product FDR**	**Limma adjusted p-value**
Q8IDQ2/ PF3D7_1343700	PfKelch13 protein, putative	11	0.63±0.09	2.63×10^{-6}*	1.1×10^{-5}	0	0	0.006
Q8I492/ PF3D7_0500800	Mature parasite-infected erythrocyte surface antigen	11	0.81±0.14	0.002	0.009	0.02	0.45	0.78
Q8IIJ9/ PF3D7_1116700	Probable cathepsin C	11	0.81±0.2	0.02	0.013	0.04	0.61	0.78
Q6ZMA7/ PF3D7_0406200	Sexual stage-specific protein	11	2.0±1.4	0.02	0.011	0	0.01	0.78
Q8IC42/ PF3D7_0702500	Uncharacterized protein	11	1.4±0.5	0.02	0.03	0.004	0.12	0.78

353

354

References

[1] WHO (**2016**) World Malaria Report. World Health Organisation. Geneva.
[2] Bhattarai A, Ali AS, Kachur SP, et al. Impact of artemisinin-based combination therapy and insecticide-treated nets on malaria burden in Zanzibar. PLoS Med **2007**;4: e309.
[3] Dondorp AM, Nosten F, Yi P, et al. Artemisinin resistance in *Plasmodium falciparum* malaria. N Engl J Med **2009**;361: 455-467.
[4] Witkowski B, Amaratunga C, Khim N, et al. Novel phenotypic assays for the detection of artemisinin-resistant *Plasmodium falciparum* malaria in Cambodia: *in-vitro* and *ex-vivo* drug-response studies. Lancet Infect Dis **2013**;13: 1043-1049.
[5] Witkowski B, Khim N, Chim P, et al. Reduced artemisinin susceptibility of *Plasmodium falciparum* ring stages in western Cambodia. Antimicrob Agents Chemother **2013**;57: 914-923.
[6] Ariey F, Witkowski B, Amaratunga C, et al. A molecular marker of artemisinin-resistant *Plasmodium falciparum* malaria. Nature **2014**;505: 50-55.
[7] Takala-Harrison S, Jacob CG, Arze C, et al. Independent emergence of artemisinin resistance mutations among *Plasmodium falciparum* in Southeast Asia. J Infect Dis **2015**;211: 670-679.
[8] Amaratunga C, Witkowski B, Dek D, et al. *Plasmodium falciparum* founder populations in western Cambodia have reduced artemisinin sensitivity *in vitro*. Antimicrob Agents Chemother **2014**;58: 4935-4937.
[9] Liu LY, Yang T, Ji J, et al. Integrating multiple 'omics' analyses identifies serological protein biomarkers for preeclampsia. BMC Med **2013**;11: 236.
[10] Ashley EA, Dhorda M, Fairhurst RM, et al. Spread of artemisinin resistance in *Plasmodium falciparum* malaria. N Engl J Med **2014**;371: 411-423.
[11] Huang F, Takala-Harrison S, Jacob CG, et al. A Single Mutation in K13 Predominates in Southern China and Is Associated With Delayed Clearance of *Plasmodium falciparum* Following Artemisinin Treatment. J Infect Dis **2015**;212: 1629-1635.
[12] Amaratunga C, Witkowski B, Khim N, Menard D and Fairhurst RM. Artemisinin resistance in *Plasmodium falciparum*. Lancet Infect Dis **2014**;14: 449-450.
[13] Straimer J, Gnadig NF, Witkowski B, et al. Drug resistance. K13-propeller mutations confer artemisinin resistance in *Plasmodium falciparum* clinical isolates. Science **2015**;347: 428-431.
[14] Fairhurst RM. Understanding artemisinin-resistant malaria: what a difference a year makes. Curr Opin Infect Dis **2015**;28: 417-425.
[15] Taylor SM, Parobek CM, DeConti DK, et al. Absence of putative artemisinin resistance mutations among *Plasmodium falciparum* in Sub-Saharan Africa: a molecular epidemiologic study. J Infect Dis **2015**;211: 680-688.
[16] Ngalah BS, Ingasia LA, Cheruiyot AC, et al. Analysis of major genome loci underlying artemisinin resistance and pfmdr1 copy number in pre- and post-ACTs in western Kenya. Sci Rep **2015**;5: 8308.
[17] Torrentino-Madamet M, Fall B, Benoit N, et al. Limited polymorphisms in k13 gene in *Plasmodium falciparum* isolates from Dakar, Senegal in 2012-2013. Malar J **2014**;13: 472.
[18] Boussaroque A, Fall B, Madamet M, et al. Prevalence of anti-malarial resistance genes in Dakar, Senegal from 2013 to 2014. Malar J **2016**;15: 347.
[19] Menard D, Khim N, Beghain J, et al. A Worldwide Map of *Plasmodium falciparum* K13-Propeller Polymorphisms. N Engl J Med **2016**;374: 2453-2464.
[20] Roper C, Alifrangis M, Ariey F, et al. Molecular surveillance for artemisinin resistance in Africa. Lancet Infect Dis **2014**;14: 668-670.
[21] Ritchie MD, Holzinger ER, Li R, Pendergrass SA and Kim D. Methods of integrating data to uncover genotype-phenotype interactions. Nat Rev Genet **2015**;16: 85-97.
[22] Trager W. Cultivation of malaria parasites. Methods Cell Biol **1994**;45: 7-26.
[23] Ahn SY, Shin MY, Kim YA, et al. Magnetic separation: a highly effective method for synchronization of cultured erythrocytic *Plasmodium falciparum*. Parasitol Res **2008**;102: 1195-1200.
[24] Paul F, Roath S, Melville D, Warhurst DC and Osisanya JO. Separation of malaria-infected erythrocytes from whole blood: use of a selective high-gradient magnetic separation technique. Lancet **1981**;2: 70-71.
[25] Dogovski C, Xie SC, Burgio G, et al. Targeting the cell stress response of *Plasmodium falciparum* to overcome artemisinin resistance. PLoS Biol **2015**;13: e1002132.

409 [26] Christophers SR, Fulton, J. D. Experiments with isolated malaria parasites (*Plasmodium knowlesi*) free
410 from red cells. Ann Trop Med Parasitol **1939**;33.
411 [27] Boersema PJ, Raijmakers R, Lemeer S, Mohammed S and Heck AJ. Multiplex peptide stable isotope
412 dimethyl labeling for quantitative proteomics. Nat Protoc **2009**;4: 484-494.
413 [28] Rappsilber J, Ishihama Y and Mann M. Stop and go extraction tips for matrix-assisted laser
414 desorption/ionization, nanoelectrospray, and LC/MS sample pretreatment in proteomics. Anal Chem
415 **2003**;75: 663-670.
416 [29] Cox J and Mann M. MaxQuant enables high peptide identification rates, individualized p.p.b.-range mass
417 accuracies and proteome-wide protein quantification. Nat Biotechnol **2008**;26: 1367-1372.
418 [30] Dallas DC, Guerrero A, Parker EA, et al. Current peptidomics: applications, purification, identification,
419 quantification, and functional analysis. Proteomics **2015**;15: 1026-1038.
420 [31] Hong F, Breitling R, McEntee CW, Wittner BS, Nemhauser JL and Chory J. RankProd: a bioconductor
421 package for detecting differentially expressed genes in meta-analysis. Bioinformatics **2006**;22: 2825-
422 2827.
423 [32] Ritchie ME, Phipson B, Wu D, et al. limma powers differential expression analyses for RNA-sequencing
424 and microarray studies. Nucleic Acids Res **2015**;43: e47.
425 [33] Creek DJ, Chua HH, Cobbold SA, et al. Metabolomics-based screening of the Malaria Box reveals both
426 novel and established mechanisms of action. Antimicrob Agents Chemother **2016**.
427 [34] Stoessel D, Nowell CJ, Jones AJ, et al. Metabolomics and lipidomics reveal perturbation of sphingolipid
428 metabolism by a novel anti-trypanosomal 3-(oxazolo[4,4-b]pyridine-2-yl)anilide. Metabolomics
429 **2016**;12.
430 [35] Creek DJ, Jankevics A, Breitling R, Watson DG, Barrett MP and Burgess KE. Toward global
431 metabolomics analysis with hydrophilic interaction liquid chromatography-mass spectrometry:
432 improved metabolite identification by retention time prediction. Anal Chem **2011**;83: 8703-8710.
433 [36] Creek DJ, Jankevics A, Burgess KE, Breitling R and Barrett MP. IDEOM: an Excel interface for analysis
434 of LC-MS-based metabolomics data. Bioinformatics **2012**;28: 1048-1049.
435 [37] Xia J, Sinelnikov IV, Han B and Wishart DS. MetaboAnalyst 3.0--making metabolomics more meaningful.
436 Nucleic Acids Res **2015**;43: W251-257.
437 [38] Zhang J, Xin L, Shan B, et al. PEAKS DB: de novo sequencing assisted database search for sensitive and
438 accurate peptide identification. Mol Cell Proteomics **2012**;11: M111 010587.
439 [39] Tilley L, Straimer J, Gnadig NF, Ralph SA and Fidock DA. Artemisinin Action and Resistance in
440 *Plasmodium falciparum*. Trends Parasitol **2016**;32: 682-696.
441 [40] Adams J, Kelso R and Cooley L. The kelch repeat superfamily of proteins: propellers of cell function.
442 Trends Cell Biol **2000**;10: 17-24.
443 [41] Mok S, Ashley EA, Ferreira PE, et al. Drug resistance. Population transcriptomics of human malaria
444 parasites reveals the mechanism of artemisinin resistance. Science **2015**;347: 431-435.
445 [42] Mbengue A, Bhattacharjee S, Pandharkar T, et al. A molecular mechanism of artemisinin resistance in
446 *Plasmodium falciparum* malaria. Nature **2015**;520: 683-687.
447 [43] Solyakov L, Halbert J, Alam MM, et al. Global kinomic and phospho-proteomic analyses of the human
448 malaria parasite *Plasmodium falciparum*. Nat Commun **2011**;2: 565.
449 [44] Krauth-Siegel RL, Muller JG, Lottspeich F and Schirmer RH. Glutathione reductase and glutamate
450 dehydrogenase of *Plasmodium falciparum*, the causative agent of tropical malaria. Eur J Biochem
451 **1996**;235: 345-350.
452 [45] Witkowski B, Lelievre J, Nicolau-Travers ML, et al. Evidence for the contribution of the hemozoin
453 synthesis pathway of the murine *Plasmodium yoelii* to the resistance to artemisinin-related drugs. PLoS
454 One **2012**;7: e32620.
455 [46] Chandra R, Tripathi LM, Saxena JK and Puri SK. Implication of intracellular glutathione and its related
456 enzymes on resistance of malaria parasites to the antimalarial drug arteether. Parasitol Int **2011**;60: 97-
457 100.
458 [47] Henriques G, Martinelli A, Rodrigues L, et al. Artemisinin resistance in rodent malaria--mutation in the
459 AP2 adaptor mu-chain suggests involvement of endocytosis and membrane protein trafficking. Malar J
460 **2013**;12: 118.
461 [48] Olszewski KL, Morrisey JM, Wilinski D, et al. Host-parasite interactions revealed by *Plasmodium*
462 *falciparum* metabolomics. Cell Host Microbe **2009**;5: 191-199.
463 [49] Lewis IA, Wacker M, Olszewski KL, et al. Metabolic QTL analysis links chloroquine resistance in
464 *Plasmodium falciparum* to impaired hemoglobin catabolism. PLoS Genet **2014**;10: e1004085.

Figure 1

Click here to download Figure Fig1_Omics_Method.tif

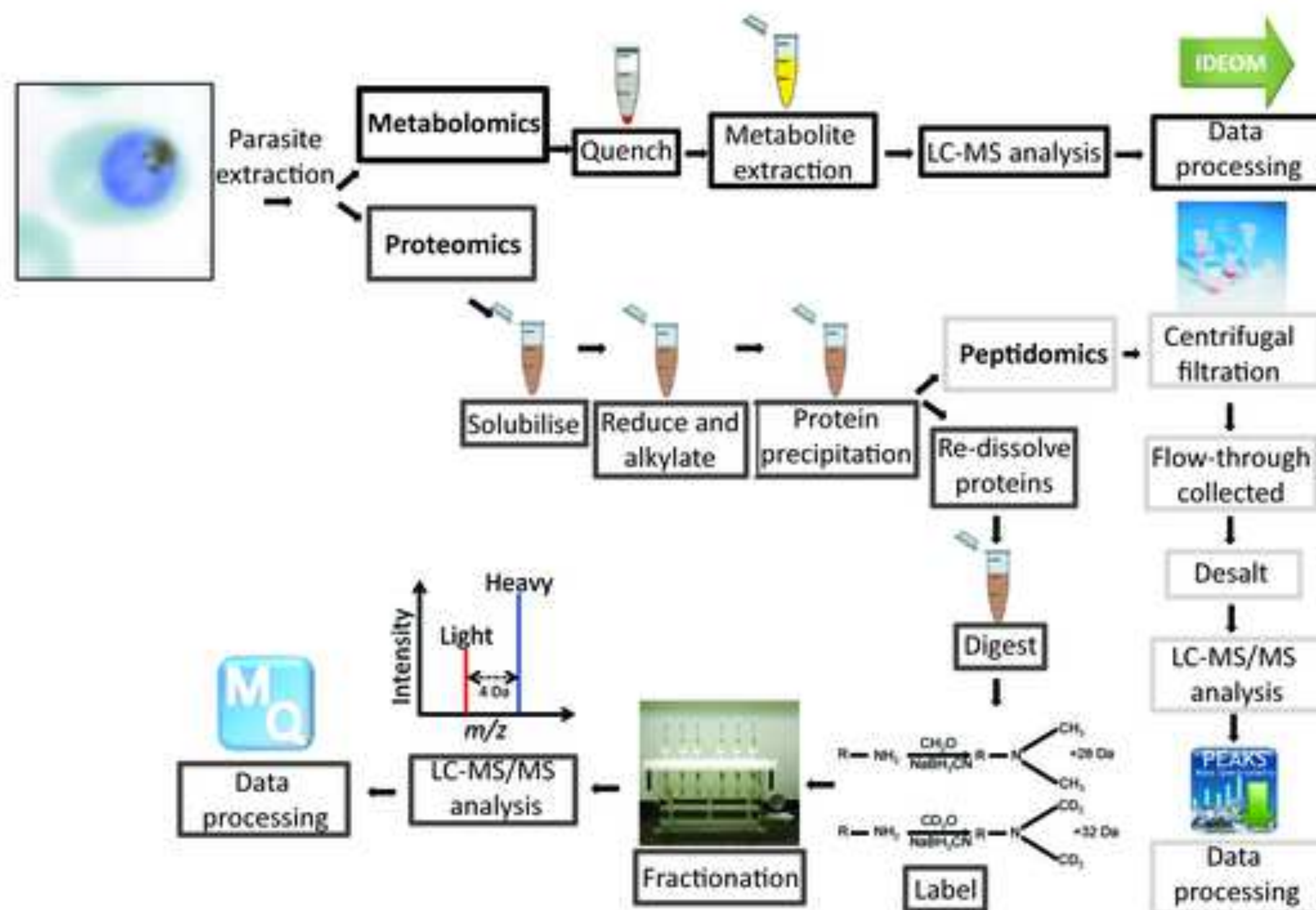

Figure 2

Click here to download Figure Fig2_Rings_volcano_plot.tif

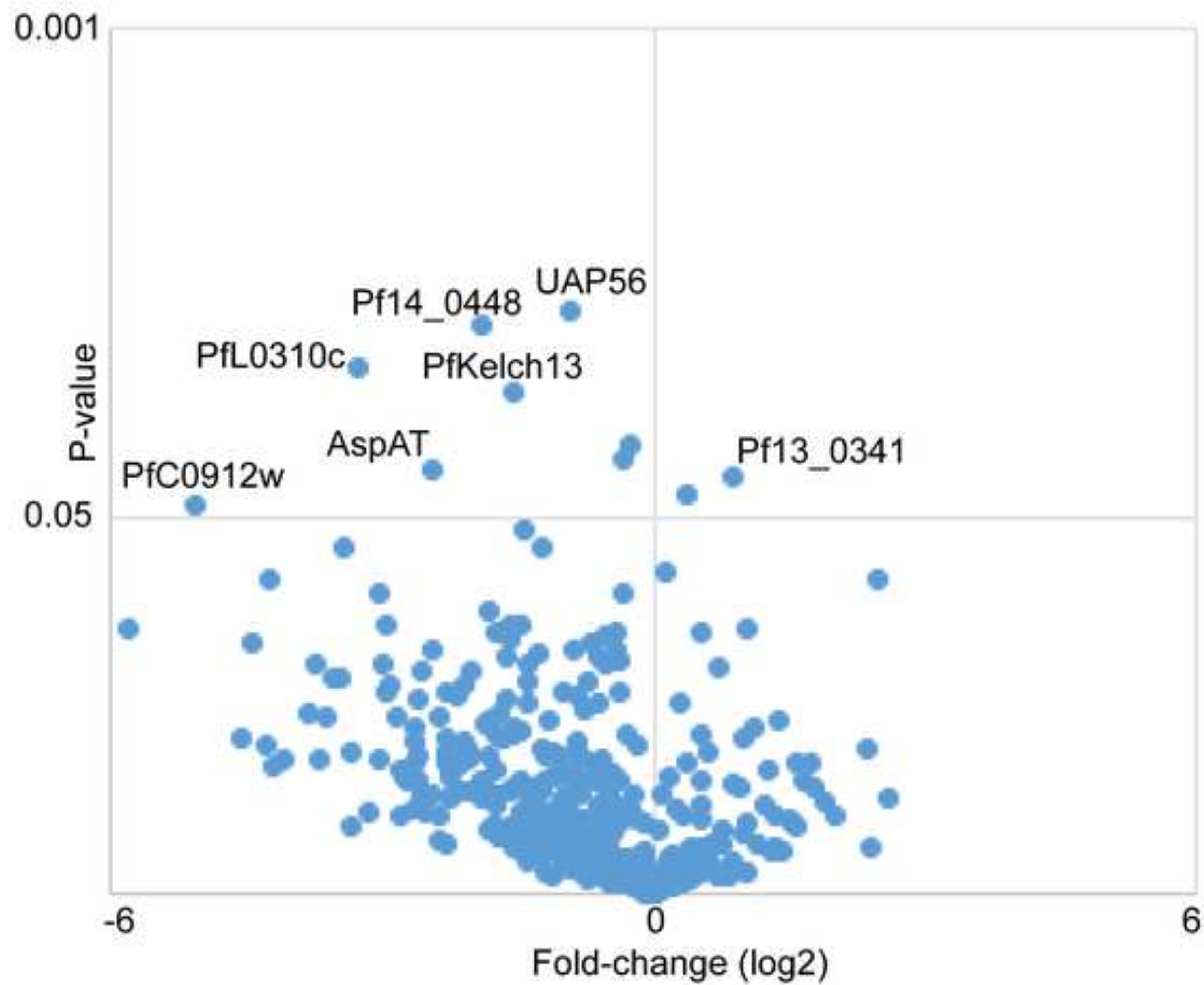

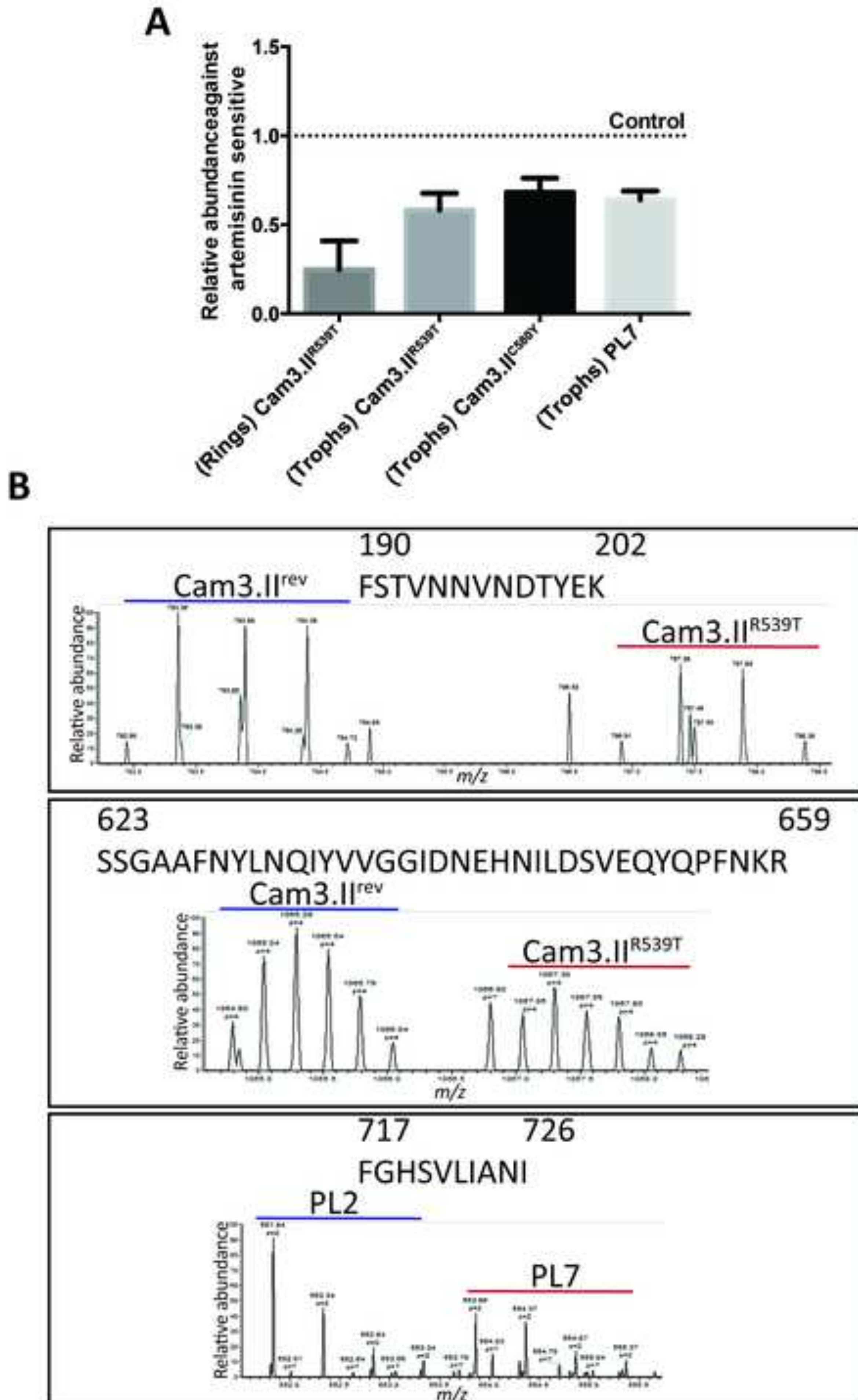
A
Relative abundance against artemisinin sensitive
1.5
1.0
0.5
0.0
Control
(Rings) Cam3.II R539T
(Trophs) Cam3.II R539T
(Trophs) Cam3.II C580Y
(Trophs) PL7
B
190
202
Cam3.II rev
FSTVNNVNDTYEK
Cam3.II R539T
Relative abundance
m/z
623
659
SSGAAFNYLNQIYVVGGIDNEHNILDSVEQYQPFNKR
Cam3.II rev
Cam3.II R539T
Relative abundance
m/z
717
726
FGHSVLIANI
PL2
PL7
Relative abundance
m/z

Figure 4

Click here to download Figure Fig4_metabolomics_pslda_foldchanges_v3.tif

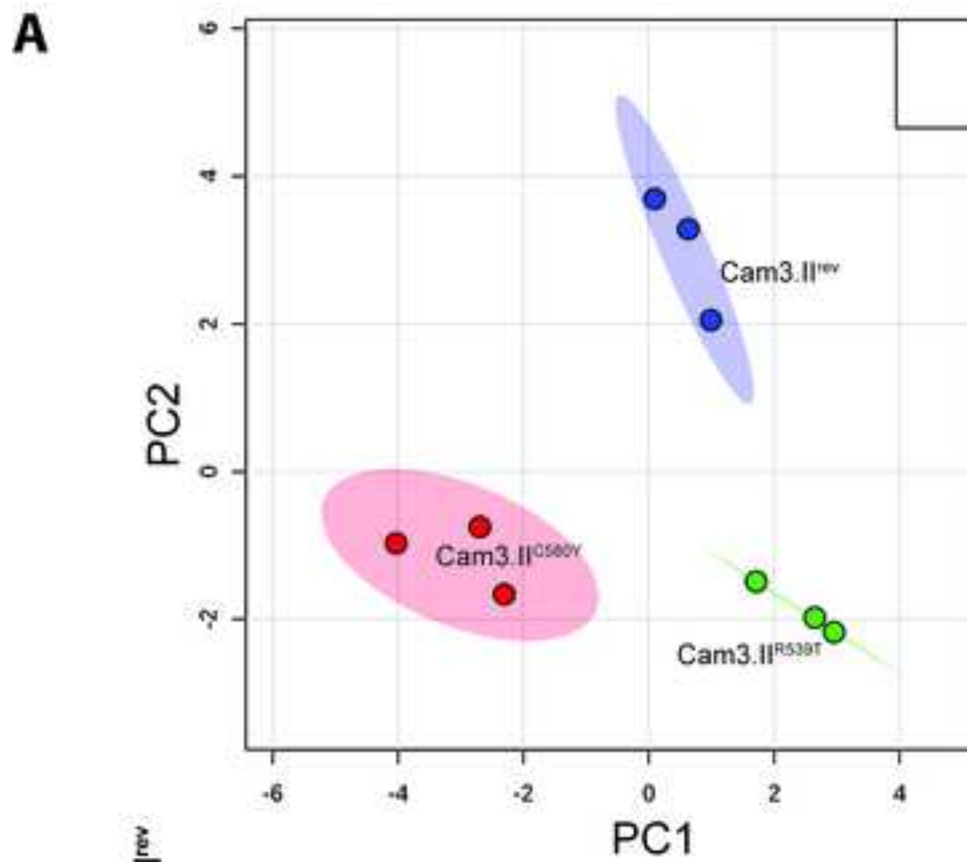

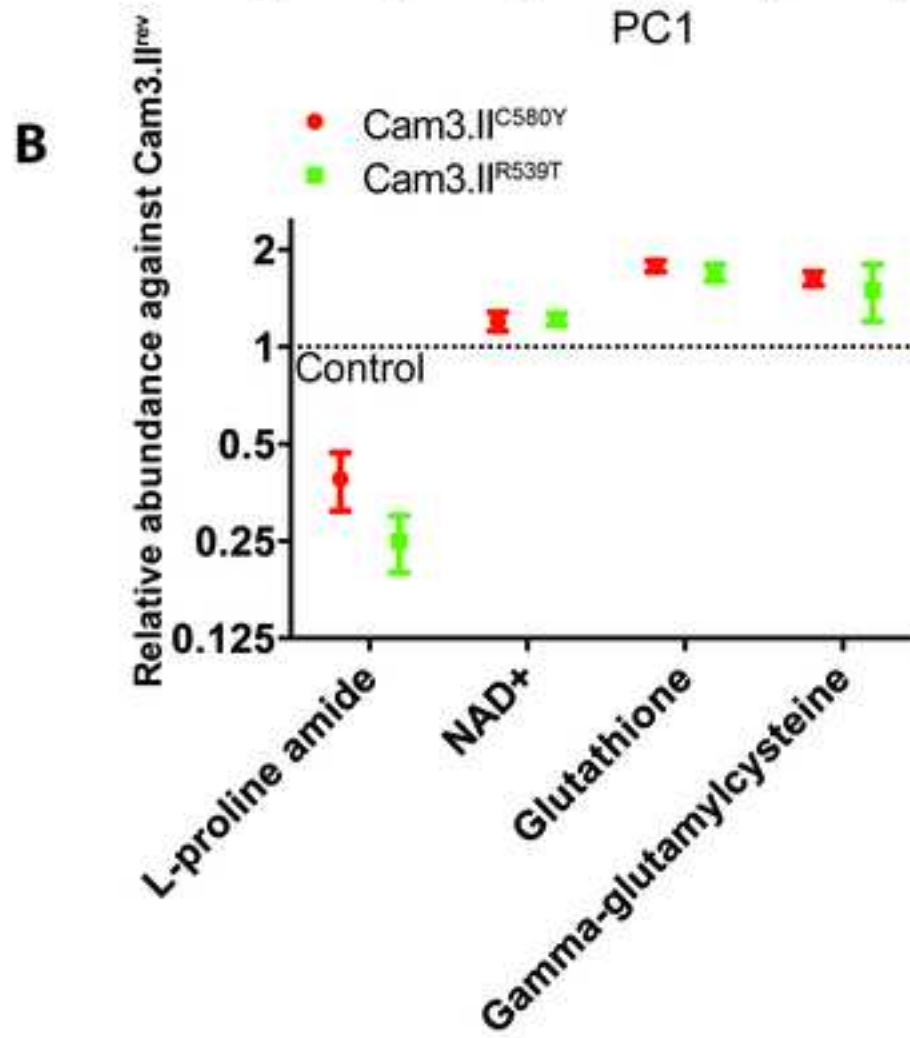

Figure 5

Click here to download Figure Fig5_Peptidomics_analysis_v3.tif